PHYSOR 2004 -The Physics of Fuel Cycles and Advanced Nuclear Systems: Global Developments
Chicago, Illinois, April 25-29, 2004, on CD-ROM, American Nuclear Society, Lagrange Park, IL. (2004)

A Comparison of Binary Stochastic Media Transport Models in "Solid-Void" Mixtures

I.M. Davis[*1], T.S. Palmer[1], and E.W. Larsen[2]
[1]*Department of Nuclear Engineering and Radiation Health Physics, Oregon State University, Corvallis, OR 97331, USA*
[2]*Department of Nuclear Engineering and Radiological Sciences, University of Michigan, Ann Arbor, MI 48109, USA*

We provide numerical comparisons of the Levermore-Pomraning and atomic mix transport models with benchmark calculations for a class of planar geometry binary stochastic media systems in which one of the two materials is a void. We show that the Levermore-Pomraning approximation is always the superior approximation for low to moderate scattering ratios in the solid material, and is competitive with atomic mix in diffusive systems of this class. We also show trends in the error of the two approximations as well as trends in the standard deviation of the benchmark ensemble-average scalar flux.

KEYWORDS: Stochastic Media, Random Media, Stochastic Mixtures, Transport

1. Introduction

The last several years have seen a resurgence of interest in improved models for the transport of particles in stochastic mixtures. [By stochastic mixtures, we mean materials whose properties at any given spatial location are known only in a statistical sense.] Several applications are driving the recent research, including neutron transport in pebble bed reactors, charged particle transport in the lung, and solar radiation transport through cloudy atmospheres.

Most materials in radiation transport calculations are treated as "atomically mixed". This means that the volume fraction of each material is used to calculate homogenized cross-sections for the mixture. The atomic mix (AM) approximation is appropriate when the mean chord length in each material is small relative to a mean free path. In some applications, such as in stochastic mixtures, the materials are not atomically mixed. To more accurately predict the particle distribution in these materials, advanced models have been developed, the most popular being the Levermore-Pomraning (LP) model [3]. Several previous studies have compared these advanced models to the results of benchmark calculations given known mixing statistics. [Benchmark calculations are computed by averaging the solutions of transport calculations for a large number of realizations of the mixing statistics.] A previous study by Adams et al. [1] compared the LP approximation to benchmark calculations for a specified set of systems in rod and planar geometry. A comparison of three different stochastic mixture models with benchmark calculations using various chord length distribution functions in planar geometry was also performed by Zuchuat et al. [2]. However, we are not aware of any study that performs a systematic comparison of atomic mix, Levermore-Pomraning, and benchmark calculations. In this study, we compare

[*] Corresponding author, Tel. 541-737-7074, FAX 541-737-0480, E-mail: davisia@engr.orst.edu

the scalar flux solution for the atomic mix (AM) and Levermore-Pomraning (LP) approximations to a benchmark ensemble-average scalar flux solution (mean scalar flux and sample standard deviation). We restrict ourselves to neutral particle transport in planar geometry where the material is a binary stochastic mixture with known mixing statistics. Further, one of the two immiscible materials of the mixture is a void. It is crucial to investigate the accuracy of these approximate models, and to consider their computational efficiency in evaluating alternative approaches to the numerical simulation of the transport systems described in the previous paragraph.

We consider the time-independent, source-free, mono-energetic, planar geometry transport equation, with isotropic scattering,

$$\mu \frac{\partial \psi(x,\mu)}{\partial x} + N(x)\sigma_t \psi(x,\mu) = \frac{N(x)\sigma_s}{2} \int_{-1}^{1} \psi(x,\mu')d\mu', \tag{1}$$

where $N(x)$ is a random function taking on two values, one of which is zero for the void material. We solve (1) with non-stochastic boundary conditions: an isotropic incident angular flux on the left and vacuum boundary on the right

$$\psi(0,\mu) = 1,\ \mu > 0; \quad \psi(X,\mu) = 0,\ \mu < 0. \tag{2}$$

2. Models

For the cases of interest, we compute scalar flux solutions for comparison in three ways: (i) a stochastic benchmark calculation, in which solutions of a large number of realizations of the mixing statistics are averaged, (ii) the atomic mix (AM) approximation [3], and (iii) the Levermore-Pomraning (LP) approximation [3]. Scalar flux solutions of both the AM and LP models approximate the mean scalar flux for a binary stochastic mixture (ensemble-average) given by the benchmark solution.

All of our calculations were performed on a 750 MHz Sun UltraSPARC™ III. The benchmark calculation is significantly more expensive computationally than either the AM or LP models. If either of these two models is sufficiently accurate, they will be preferable to the benchmark calculation. The benchmark code run time with 10,000 realizations was observed to take as long as 52 minutes for thick, absorbing systems and 64 minutes for thick, diffusive systems. For comparison, the LP approximation run time for these same cases took on the order of 10 seconds for thick, absorbing systems, and 20 seconds for thick, diffusive systems. The AM calculations finished in approximately one second for both of these systems. All of the reported time estimates are wall clock time.

The goal is to approximate the benchmark ensemble-average scalar flux accurately and inexpensively using an approximate model -- such as AM or LP. In this paper, we compare these three techniques for estimating this ensemble-average scalar flux, in order to assess the accuracies of the AM and LP approximations. We also give some numerical estimates of the standard deviation of the scalar flux about the mean; this quantity is not estimated by any known theory at the present time.

2.1 Mixing Statistics

Markovian mixing statistics were used in this study, although Adams et al. [1] have derived two coupled statistical transport equations for binary stochastic media with arbitrary mixing statistics, so one need not be restricted to this statistical distribution. Markovian statistics dictate that the chord lengths in the materials satisfy an exponential distribution:

$$f_i(\xi) = \lambda_i^{-1} \exp(-\xi/\lambda_i), \tag{3}$$

where the probability of any random material segment length [$f_i(\xi)d\xi$] lying between ξ and $\xi + d\xi$, is $\lambda_i^{-1} \exp(-\xi/\lambda_i)$ and λ_i is the mean segment length in material i [1].

Zuchuat et al. [2] have shown previously that, in systems of small length, the probability of reflection and transmission does not vary with mixing statistics in planar geometry. They postulated that this is due to the fact that there are few material interfaces in a system of small length, which weakens the importance of the mixing distribution type. Zuchuat et al. [2] also observed that only in systems on the order of 10 cm or greater do the mixing statistics become influential to reflection and transmission probabilities. We can therefore say with some confidence that the trends that we infer from the data generated using Markov statistics in the benchmark and LP equations should be representative of the mixing in [2] for thin systems. We cannot conclude that these trends are present for different mixing statistics in systems of greater length.

2.2 Benchmark Calculation

The benchmark calculation has both a stochastic and deterministic component, resulting in an ensemble-average or mean scalar flux and associated sample standard deviation determined by many individual realizations of the mixing statistics. For stochastic media transport systems, the mixing statistics are an (assumed) known distribution of volume averaged interfacial areas between the two materials composing the mixture. The material statistics are homogenous in each of the two disparate materials in the mixture. In planar geometry this simplifies to a distribution of mean chord lengths between two materials denoted by $\lambda_i; i = 0,1$. The mixing statistics were taken to be a Markovian distribution, which is sampled to gain a material width (x_i) of one of the two materials $x_i \in X, i = 0,1$, where X is the system length. The distribution is sampled for widths of alternating material in this stochastic fashion until the entire system is populated. After this single realization of the system is generated, the solution is obtained deterministically, by solving (1) with the diamond-difference spatial discretization and the discrete ordinates angular approximation with non-stochastic boundary conditions (2). Mesh sizing for the system was restricted to

$$\Delta x \le (1/5)|\mu|_{\min} / \Sigma_{ti} \tag{4}$$

as in [1] where $\mu_{\min}$ is the minimum ordinate in the quadrature set. If a material region is larger than the minimum mesh spacing given by (4), it is broken into spatial cells of the minimum mesh spacing. If the material region is smaller than the minimum mesh spacing, the region is treated as a single spatial cell. This causes the cell centers to lie at different locations for each realization. The converged scalar flux solution is interpolated to a common spatial mesh so that a mean (ensemble-average) and sample standard deviation of the

scalar flux over all realizations can be calculated using

$$s = \left\{ \left(\frac{1}{R} \sum_{n=1}^{R} \phi_n(x)^2 \right) - \bar{\phi}(x)^2 \right\}^{1/2}, \tag{5}$$

where $\phi_n(x)$ is a scalar flux solution of an individual realization, $\bar{\phi}(x)$ is the mean scalar flux, and R is the total number of realizations. The mesh spacing of the interpolated mesh was chosen to be small enough so as not introduce a significant error into the calculation. A 16-point Gauss-Legendre quadrature set was used in the discrete ordinates angular approximation for each realization.

A total of seven parameters can be varied in the development of a test matrix: the system length (X), the mean chord length in each material ($\lambda_i; i = 0,1$), and the total and scattering non-stochastic cross sections in the each material $(\Sigma_{ti}, \Sigma_{si}; i = 0,1)$. All of these calculations were accelerated with Larsen's 4-Step Diffusion Synthetic Acceleration (DSA) procedure [5], which is necessary to obtain a solution for diffusive systems.

After some investigation, it was found that using between 10,000 and 30,000 realizations was sufficient for converged statistics. Benchmark solutions of the mean reflection and transmission probabilities $(\langle R \rangle, \langle T \rangle)$ and associated standard deviations from [1] were reproduced very accurately using 30,000 realizations versus 100,000 realizations in [1]. Converged statistics were also checked by rerunning some cases from [1] with 50,000 and 100,000 realizations and comparing to solutions using 10,000 realizations. The largest difference observed in the mean between 10,000 and 100,000 realizations was 5.4% and 2.7% in the standard deviation.

2.3 Atomic Mix Approximation

The same code used in the benchmark calculations was used to generate solutions with the atomic mix approximation. Homogenized cross sections were generated by a volume average of the cross sections in each material

$$\overline{\Sigma} = p_i \Sigma_i + p_j \Sigma_j; i = 0,1;\ i \neq j, \tag{6}$$

where $(p_i; i = 0,1)$ are the transition probabilities, or the probability of finding the respective material at any point in the system

$$p_i = \lambda_i / (\lambda_0 + \lambda_1); i = 0,1. \tag{7}$$

This yields a system with homogeneous material characteristics, and the scalar flux solution can be obtained from a single realization. Mesh spacing was again restricted as in (4) and a 16-point Gauss-Legendre quadrature set was used in the discrete ordinates angular approximation. This single calculation was also accelerated with Larsen's 4-Step DSA [5].

2.4 Levermore-Pomraning Approximation

We consider the time-independent, source-free, mono-energetic Levermore-Pomraning equations for Markov mixing statistics as an approximation to (1),

$$\mu\frac{\partial\psi_i}{\partial x}+\Sigma_i\psi_i(x,\mu)=\frac{\Sigma_{si}}{2}\int_{-1}^{1}d\mu'\psi_i(x,\mu')+\frac{|\mu|}{\lambda_i}\left[\psi_j(x,\mu)-\psi_i(x,\mu)\right];\ i=0,1;\ i\neq j\,, \tag{8}$$

with non-stochastic boundary conditions as in (2), but prescribed to each material in the mixture,

$$\psi_i(0,\mu)=1,\ \mu>0;\quad \psi_i(X,\mu)=0,\ \mu<0;\quad i=0,1\,. \tag{9}$$

This coupled set of transport equations gives an estimate for the ensemble-average scalar flux through the transition probabilities (7) by,

$$\bar{\phi}=p_0\phi_0+p_1\phi_1\,. \tag{10}$$

The diamond-difference spatial discretization with a mesh spacing restriction as in (4) was used along with a 16-point Gauss-Legendre quadrature in the discrete ordinates angular approximation to calculate LP estimates of the ensemble-average scalar flux. As in the benchmark case, LP solutions of the mean reflection and transmission probabilities (<R>, <T>) and associated standard deviations from [1] were reported very accurately using 30,000 realizations versus 100,000 realizations in test cases from [1]. The same seven parameters which were varied in the benchmark and AM calculations were again used to generate solutions for the cases of interest for this study. The calculation was accelerated with a two-grid acceleration scheme developed by Ching [6].

3. Analysis

As previously mentioned, there are seven variable parameters to consider in the analysis of binary stochastic media transport systems with Markovian mixing statistics in planar geometry when calculating a benchmark, LP, or AM scalar flux solution. When one of the materials in the mixture is void, $\left(\Sigma_{t_{Void}}=\Sigma_{s_{Void}}=0\right)$ this number is reduced to five. We consider those systems relevant to pebble-bed reactors, which reduces the number of parameters further. Two sets of systems were considered, each with a varying number of cases. Set 1 contained 36 cases where the mean chord length and total cross section of the solid material were set to unity $\left(\lambda_{Solid}=1cm;\Sigma_{t_{Solid}}=1cm^{-1}\right)$. Set 2 contained 27 cases where the mean chord length of the solid was set to 0.5 and the total cross-section was set to unity $\left(\lambda_{Solid}=0.5cm;\Sigma_{t_{Solid}}=1cm^{-1}\right)$. These mean chord lengths and optical thicknesses of the solid material are representative of the fuel spheres of a pebble-reactor, and the mean chord length of the void is representative of the coolant. This reduces the degrees of freedom in the analysis, and results in only three variable parameters ($\Sigma_{s_{Solid}}$, λ_{Void}, X). Table 1 shows the values used for these variable parameters in the analysis where the subscript "0" denotes the solid material of the mixture and "1" denotes the void material.

Table 1 Sets of Calculation Cases

Set Parameters	**Set 1**	**Set 2**
	$\lambda_0 = 1$ cm , $\Sigma_{t0} = 1$ cm^{-1}, $\Sigma_{s0} = C_0$ $\lambda_1 = L$, $\Sigma_{t1} = \Sigma_{s1} = 0$ cm^{-1}	$\lambda_0 = 0.5$ cm , $\Sigma_{t0} = 1$ cm^{-1}, $\Sigma_{s0} = C_0$ $\lambda_1 = L$, $\Sigma_{t1} = \Sigma_{s1} = 0$ cm^{-1}
C_0	0.1, 0.5, 0.99 cm^{-1}	0.1, 0.5, 0.99 cm^{-1}
L	0.05, 0.1, 1, 2 cm	$(\lambda_0/3)$, λ_0, $(3\lambda_0)$ cm
X	5, 10, 100 cm	5, 10, 100 cm
Number of Cases	36	27
Realizations	10,000	10,000

The 63 cases considered were each calculated using the three models described above: benchmark, AM, and LP.

4. Numerical Results

In the benchmark calculation, the sample standard deviation and the mean were calculated at each of the zone centers of the interpolation mesh. It was found that in all cases the AM and LP approximations did lie well within $\pm 2\sigma$ of the mean. Since the incident angular flux is known from the boundary conditions (2) and (9) (angular flux is known for all directions incident on the system) the sample standard deviation is smaller at the boundaries of the system and is a maximum near the center of the system. There is usually much more variation in the solution near the right edge of the system than at the left edge, due to the number of material interfaces encountered in the interior. This generally results in a minimum standard deviation located at the left edge of the system. Figure 1, 2 and 3 are representative plots of the AM and LP approximations to the benchmark mean, with $\pm 2\sigma$ sample standard deviation of the benchmark mean, as well as solutions to individual realizations for scattering ratios $\left(\Sigma_{s_{Solid}} / \Sigma_{Solid}\right)$ of 0.1, 0.5, and 0.99, respectively.

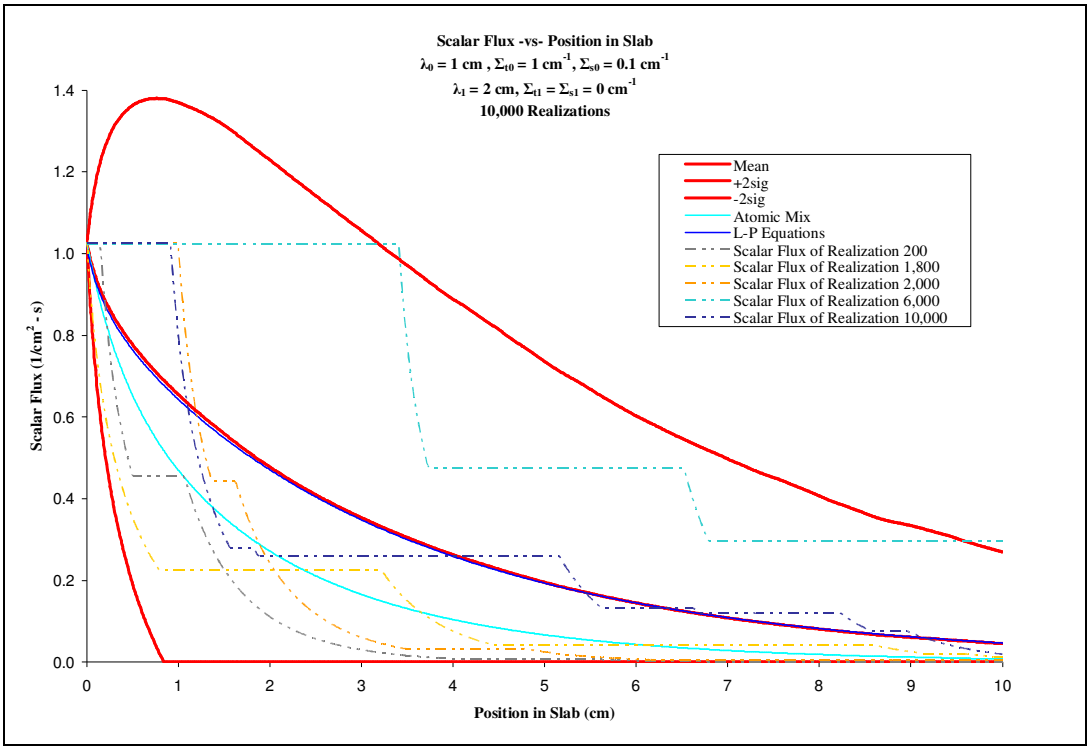

Fig. 1 LP and AM approximations to a benchmark ensemble average scalar flux, also showing five solutions of independent realizations of the benchmark.

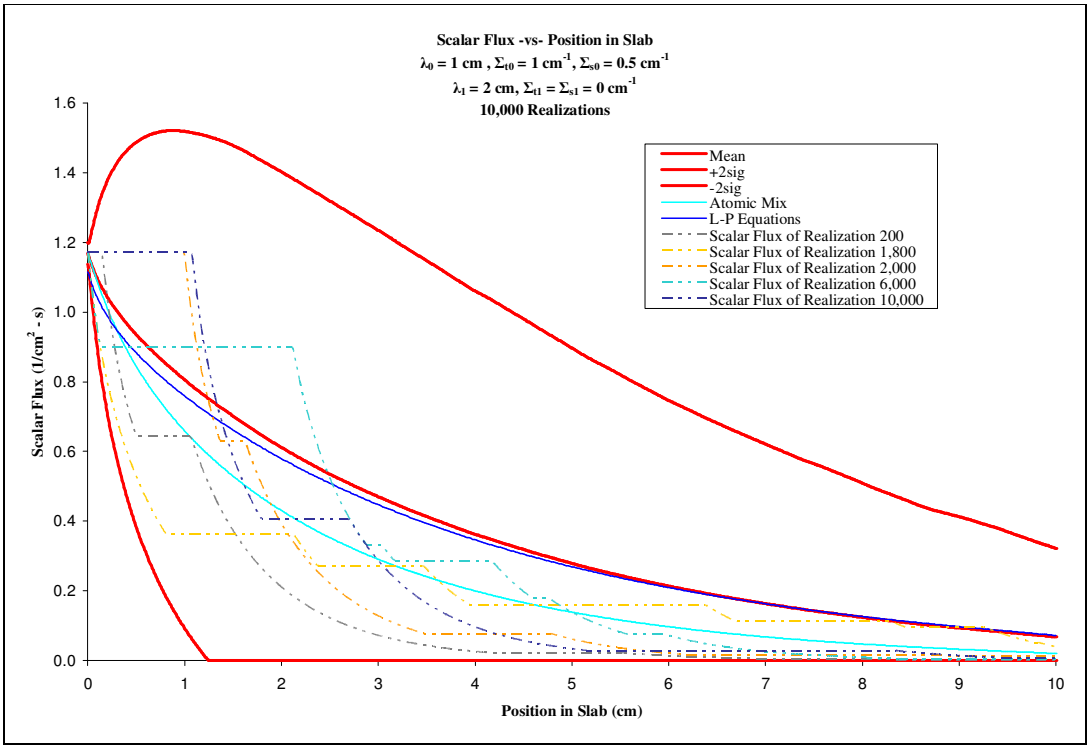

Fig. 2 LP and AM approximations to a benchmark ensemble average scalar flux, also showing five solutions of independent realizations of the benchmark.

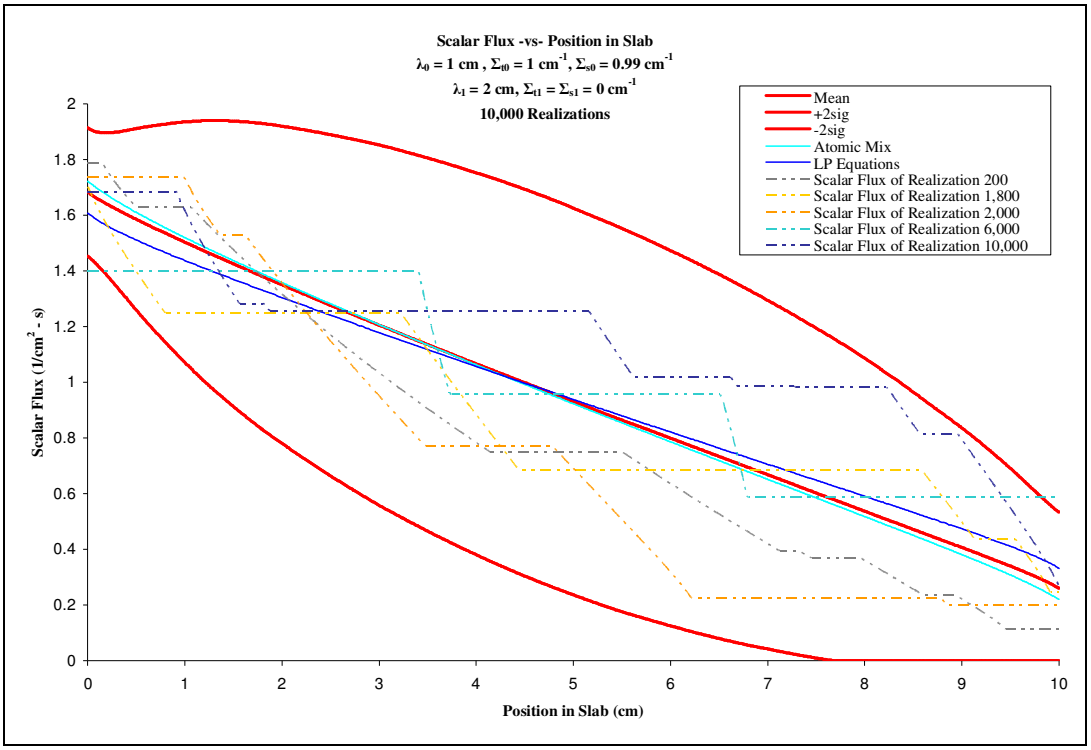

Fig. 3 LP and AM approximations to a benchmark ensemble average scalar flux, also showing five solutions of independent realizations of the benchmark.

Inspection of the individual realization scalar flux solutions will reveal a flat solution across void regions, as expected. Figures 1, 2, and 3 show a general trend found in all of the plots: for systems with a low to moderate scattering ratio (0.1 or 0.5), the LP approximation is much more accurate than the AM approximation, while at scattering ratios close to unity, the AM and LP approximations are competitive. This is especially true in systems where the ratio of mean chord lengths $(\lambda_{Void}/\lambda_{Solid})$ was large. We will clarify this in subsections below.

Several important trends are evident when comparing the scalar flux solutions from the AM model and LP model with the benchmark. The trends we explore are: i) the variation of the relative error of the benchmark, LP, and AM approximations and ii) the variation of the standard deviation of the benchmark with changes in the three variable parameters $(\Sigma_{s_{Solid}}, \lambda_{Void}, \mathrm{X})$.

4.1 Relative Error of the LP and AM Approximation with the Benchmark

The relative LP approximation error and the relative AM approximation error were compared. These respective relative errors were calculated by,

$$LP_{\mathrm{Re}lative\ Error} = \frac{\left|\phi(x)_{LP} - \phi(x)_{Benchmark}\right|}{\phi(x)_{Benchmark}} \tag{11}$$

$$AM_{\mathrm{Re}lative\ Error} = \frac{\left|\phi(x)_{AM} - \phi(x)_{Benchmark}\right|}{\phi(x)_{Benchmark}}. \tag{12}$$

Plots of these relative errors are given in Figures 4, 5, and 6 for selected systems where the ratio of mean chord lengths is large.

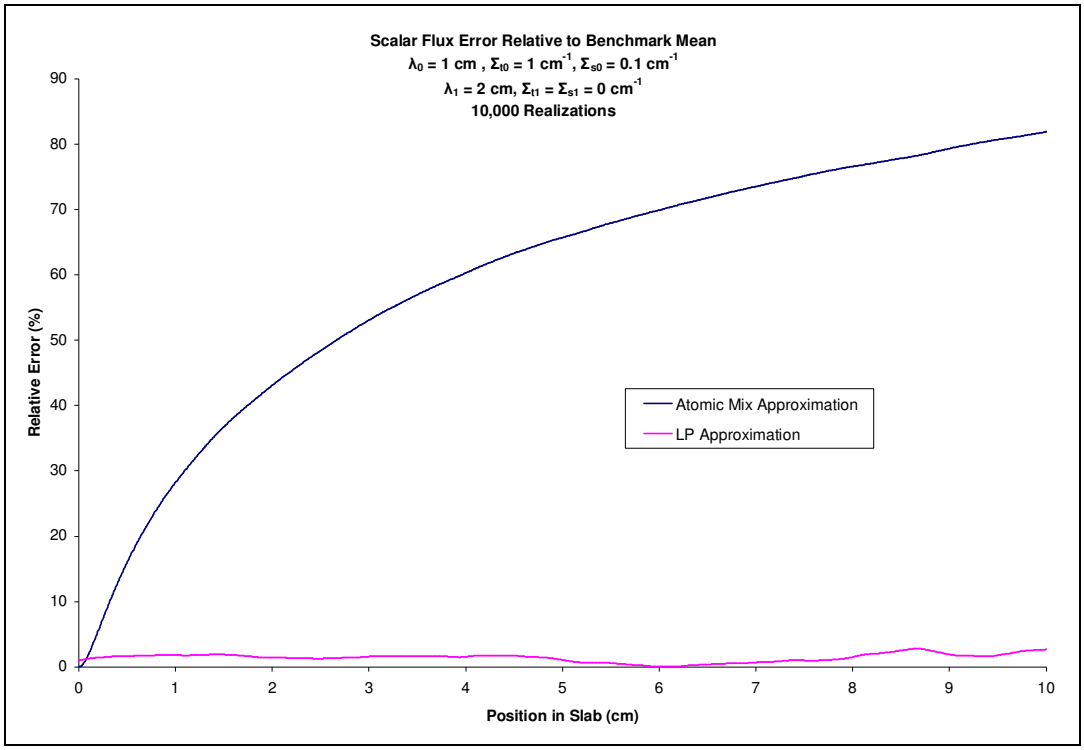

Fig. 4 Relative error of the LP and AM approximations to the benchmark ensemble-average.

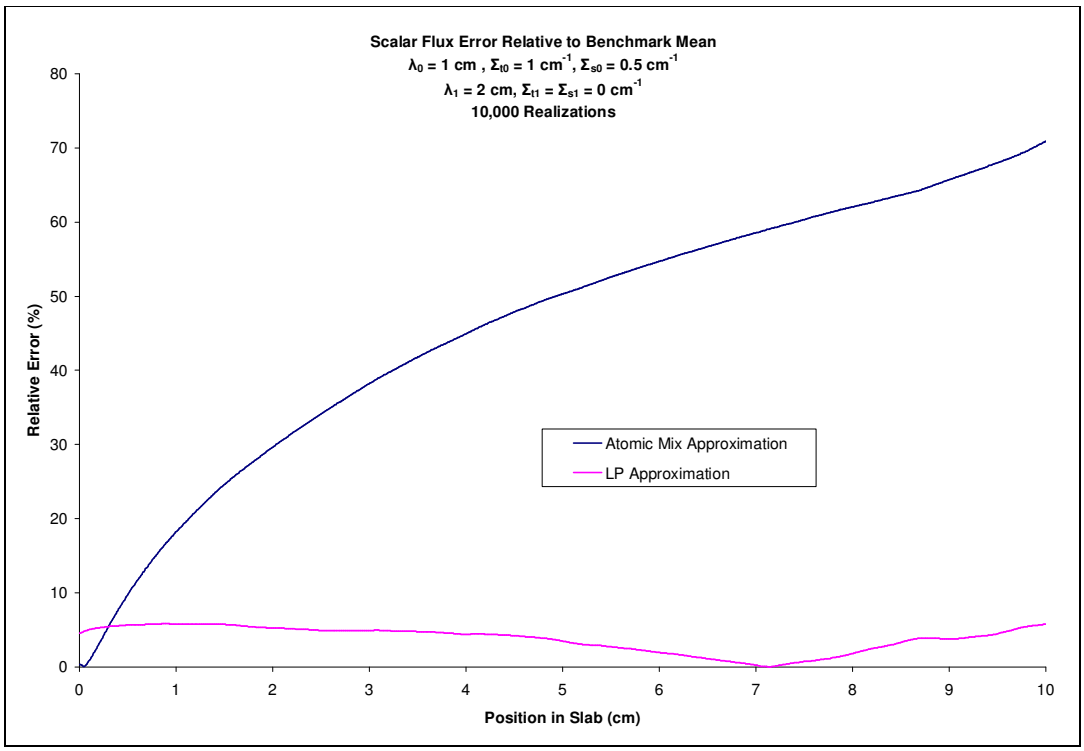

Fig. 5 Relative error of the LP and AM approximations to the benchmark ensemble-average.

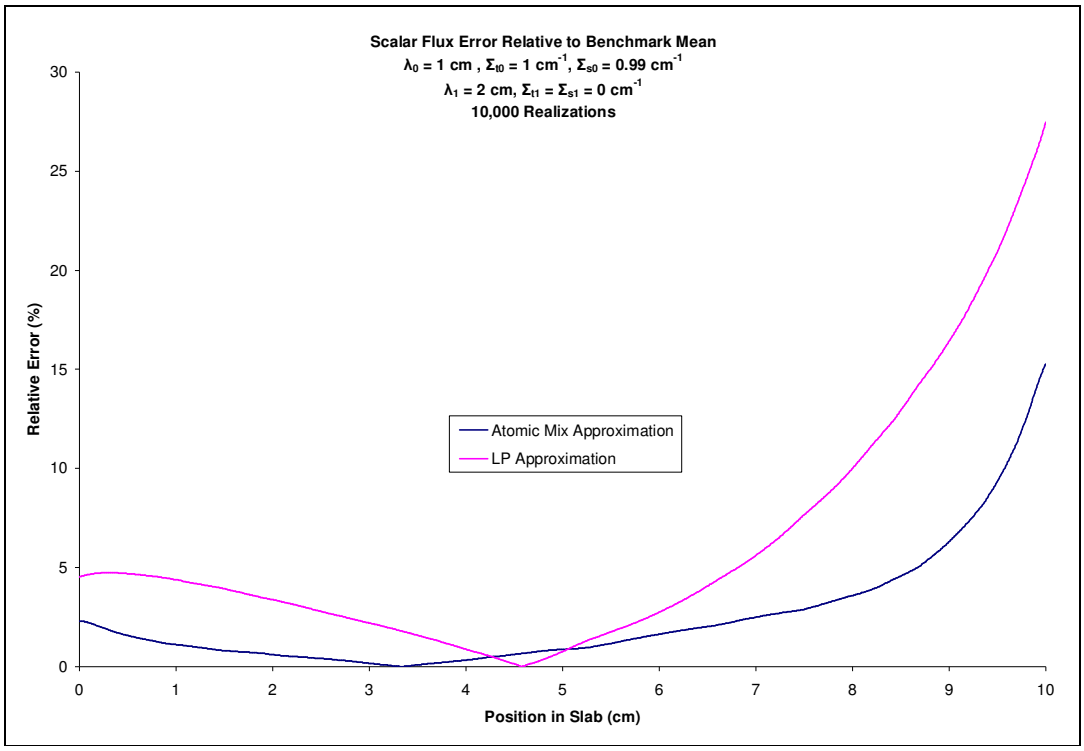

Fig. 6 Relative error of the LP and AM approximations to the benchmark ensemble-average.

These are representative of the trends found for the AM and LP approximations in all the test cases: LP is the superior model for low to moderate scattering ratios. As the scattering ratio approaches unity the accuracy of the AM approximation improves while the LP approximation begins to degrade, particularly for systems in which the mean chord length ratio is large. However, in these diffusive cases, the magnitude of the relative error of the LP approximation is comparable to that of AM.

Figure 7, 8, and 9 are plots of systems of the same lengths and scattering ratios as in Figures 4, 5, and 6, but with a smaller mean chord length ratio. While the trends discussed in the previous paragraph are still evident, the magnitude of the relative error is much smaller than in Figures 4, 5, and 6.

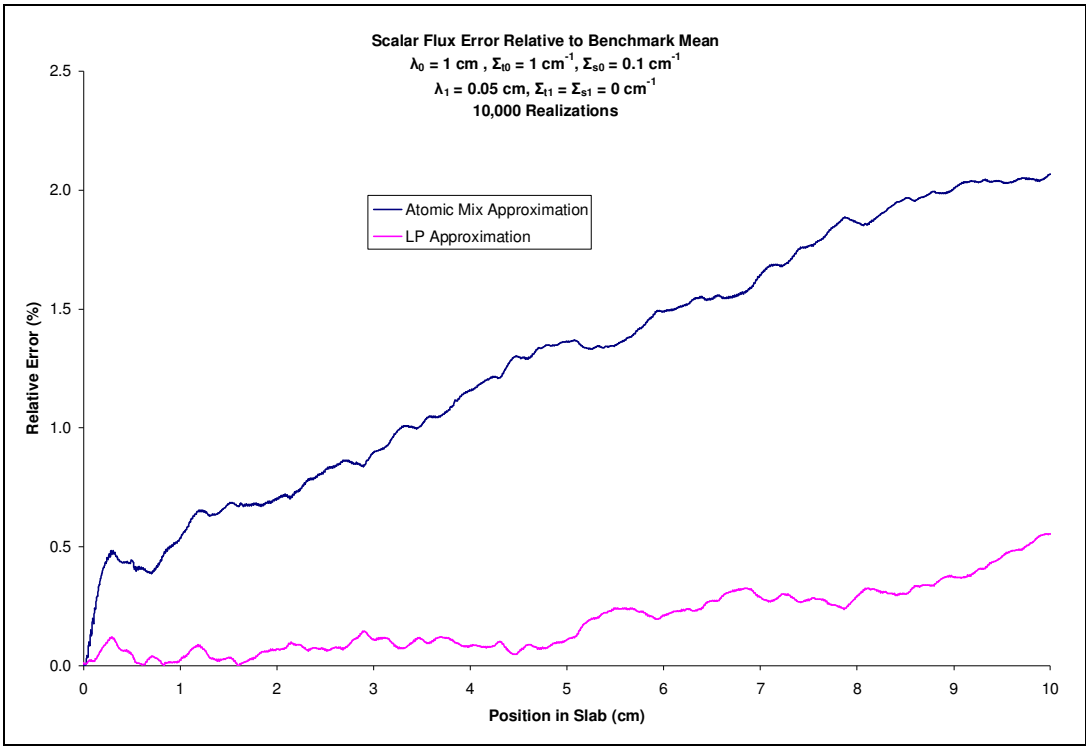

Fig. 7 Relative error of the LP and AM approximations to the benchmark ensemble-average.

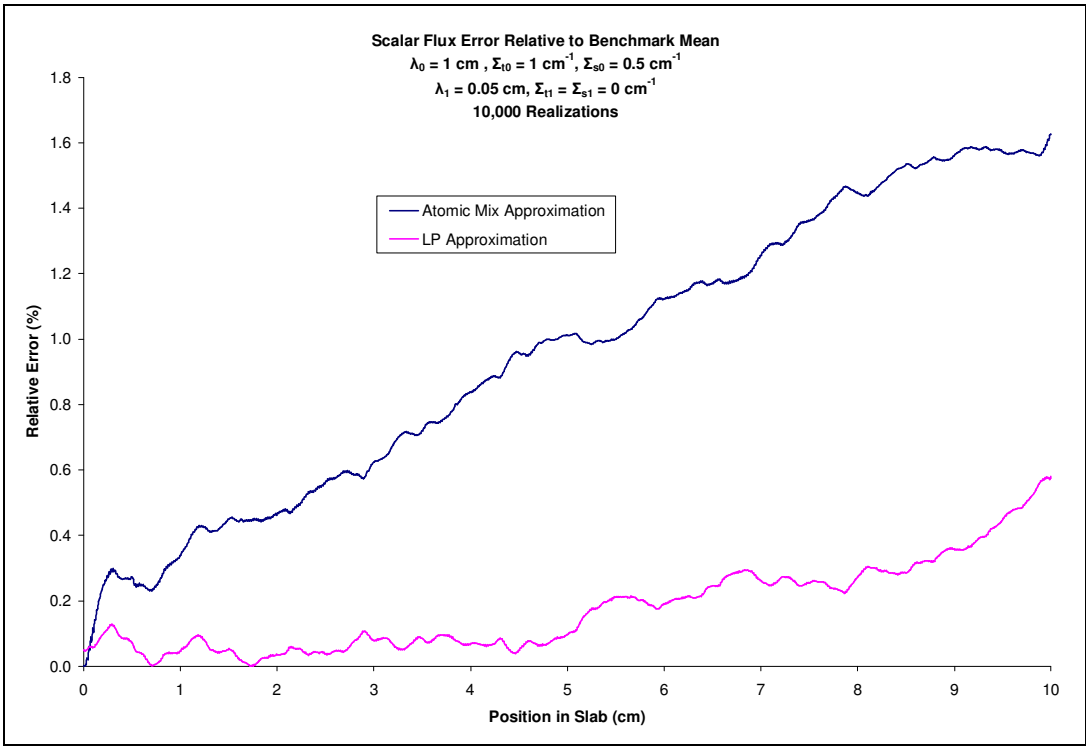

Fig. 8 Relative error of the LP and AM approximations to the benchmark ensemble-average.

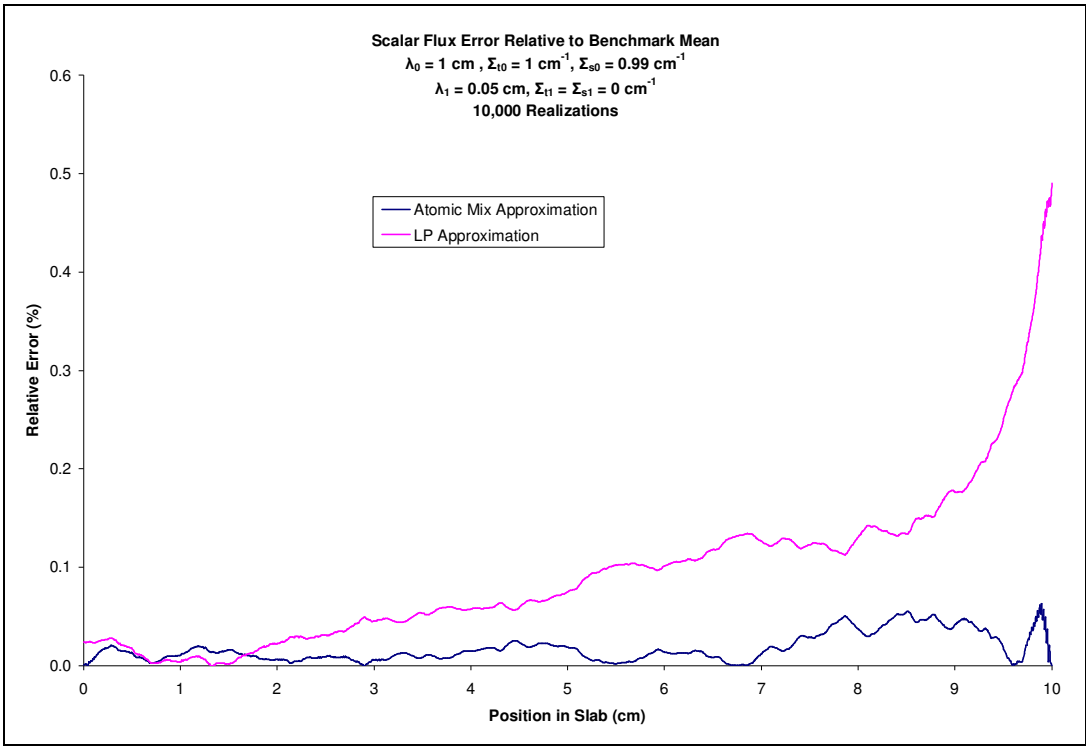

Fig. 9 Relative error of the LP and AM approximations to the benchmark ensemble-average.

The shape of these curves is governed by the scattering ratio, while the magnitude of the relative error is governed by the mean chord length ratio. On as small of a scale as in Figures 7, 8, and 9, the curves show some oscillatory behavior due to the stochastic nature of the benchmark calculation. On a larger scale as in Figures 4, 5, and 6, this behavior would be smoothed out, but the curves would be barely visible, if at all.

Figures 10 (a) – (h) and Figures 11 (a) – (f) show plots of the Euclidean norm of the relative error of the LP and AM approximations as functions of ratios of the variable parameters. Figures 10 (a) – (h) show plots of the relative error of the LP and AM approximations for a variety of mean chord length ratios as a function of the system length ratio $\left(X / X_{Max}\right)$, where X_{Max} is the maximum system length explored, 100 cm.

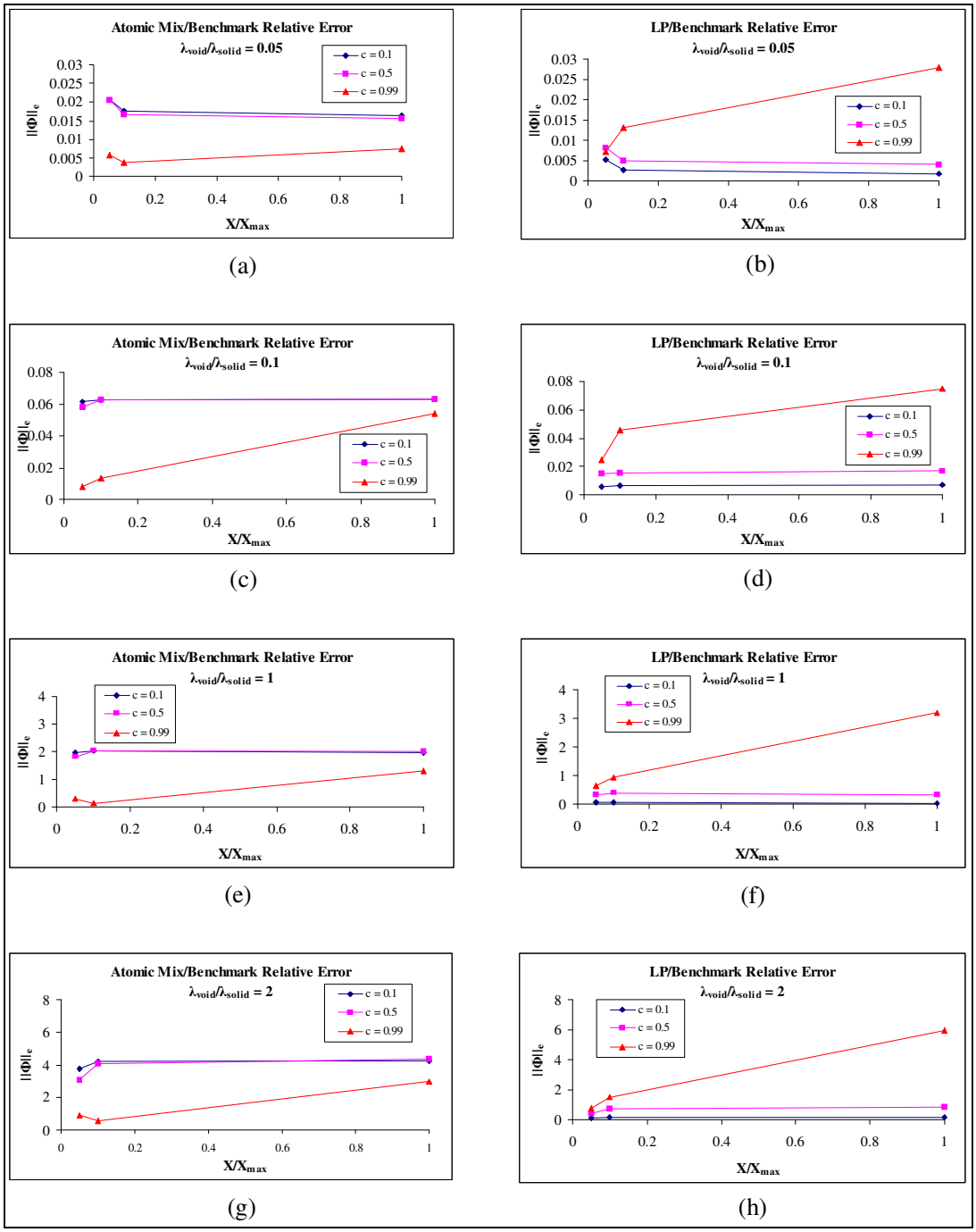

Fig. 10 (a) – (h) Euclidean norms of the relative error for a given mean chord length ratio.

The norms for both approximations are relatively flat as the system length ratio increases, showing insensitivity of the relative error to system size. For both methods the relative error is very flat for low to moderate scattering ratios. The size of the mean chord length ratio has a profound effect on the magnitude of the norm of the relative error for both approximations (Figures 10 (a) – (h)) , top to bottom).

As the scattering ratio approaches unity, another trend becomes evident for both approximations. For a given mean chord length ratio (Figures 10 (a) – (h)), left and right

neighboring plots), a higher scattering ratio in the AM approximation gives a lower relative error, while a higher scattering ratio in the LP approximation gives a higher relative error. The magnitude of the LP and AM relative error norms in diffusive systems are similar, but the LP relative error norm is much lower for low to moderately diffusive systems.

These same trends can be noted when viewing Figures 11 (a) – (f). Here we plot the norm of the relative error for both approximations as a function of mean chord length ratio for specific system sizes.

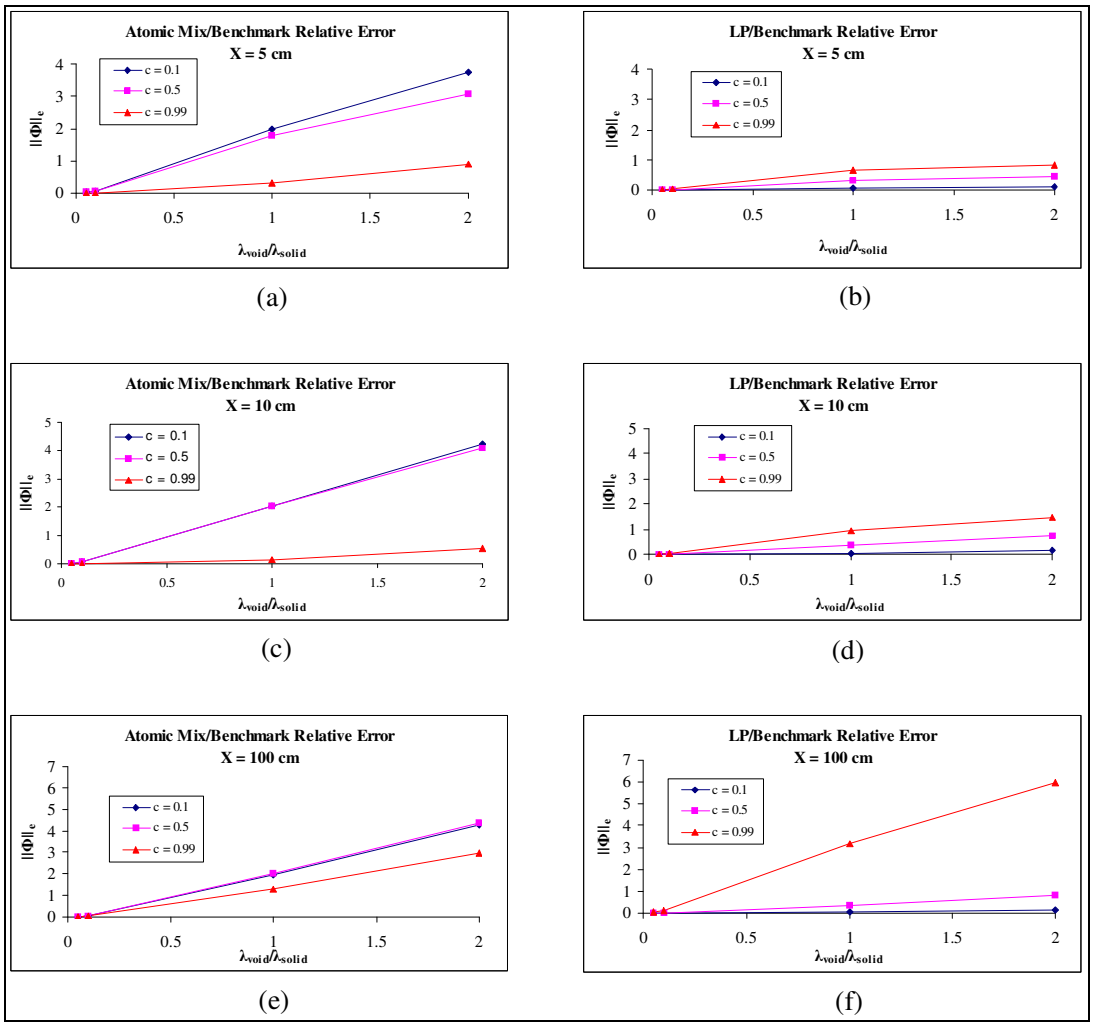

Fig. 11 (a) – (f) Euclidean norms of the relative error for a given system length.

It should be noted that Figures 10 (a) – (h) and Figures 11 (a) – (f) show only those cases from Set 1 (Table 1). Similar plots were generated for those cases in Set 2, but were omitted because the trends were identical but shifted in magnitude.

4.2 Sample Standard Deviation of the Ensemble-Average Scalar Flux

Figures 12 (a) – (d) and Figures 13 (a) – (c) show the Euclidean norm of the sample standard deviation of the benchmark scalar flux as a function of the system length ratio for given mean chord length ratios.

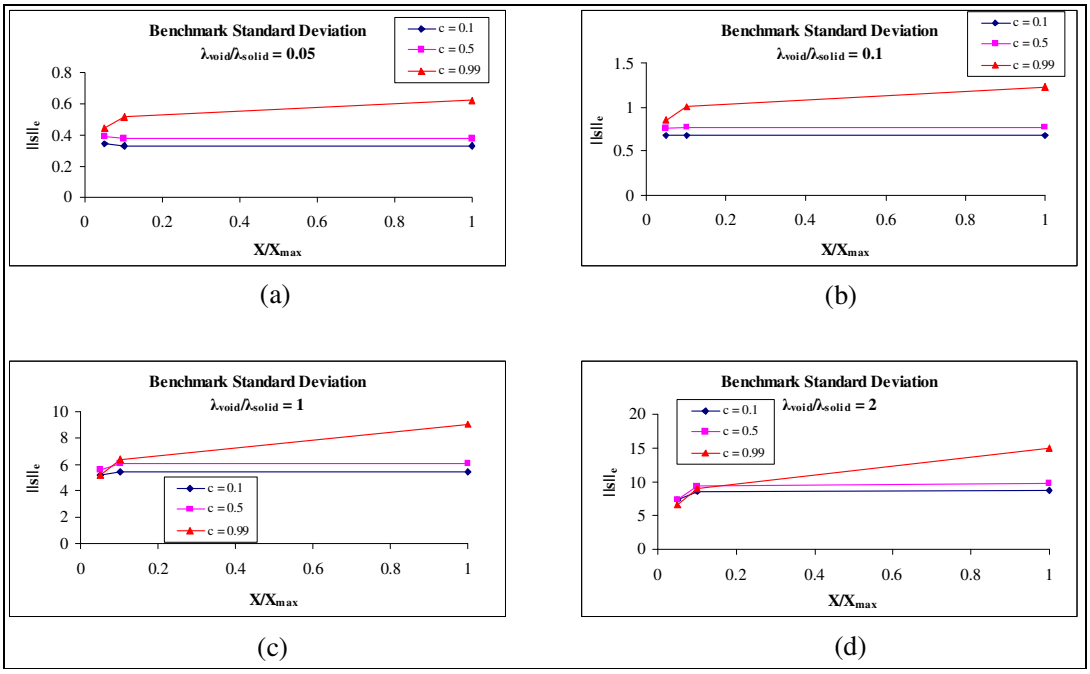

Fig. 12 (a) – (d) Euclidean norms of the benchmark standard deviation for a given mean chord length ratio.

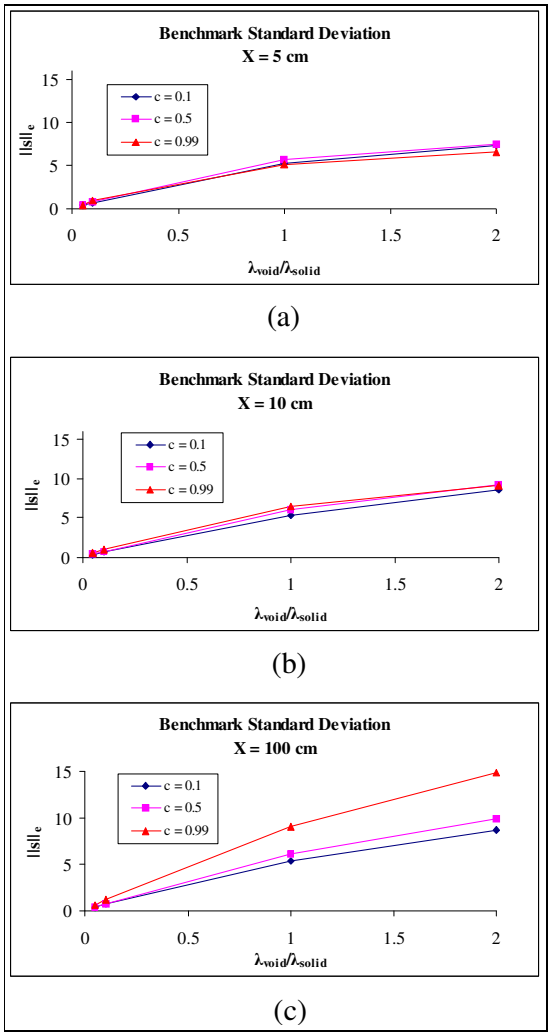

Fig. 13 (a) – (c) Euclidean norms of the benchmark standard deviation for a given system length.

These plots show the standard deviation is insensitive to system length for any given mean chord length ratio (Figures 12 (a) – (d), top to bottom). For long, diffusive systems with larger mean chord length ratios, the sample standard deviation is greatest. Figures 13 (a) – (c) show the sample standard deviation of the benchmark scalar flux as function of mean chord length ratio for a given system size. The increase in standard deviation is nearly linear with mean chord length ratio. Similar plots were generated for the trends in the standard deviation of those cases in Set 2, but were omitted because the observed trends were identical.

5. Conclusions

In general, if a single model must be chosen, then LP should be used to model this class of binary stochastic media transport systems. LP is always an improvement over AM in systems where the solid material is absorptive or mildly diffusive for the entire range of mean chord length ratios. For highly diffusive systems the LP and AM approximations are comparably inaccurate. Thick and highly diffusive systems would be found in Pebble bed type reactors, so for LP to be useful model of this stochastic system, an improvement to these equations is necessary to accurately calculate the ensemble-average scalar flux in this limit.

Models being developed to predict the standard deviation or variance of these types of systems, should accurately approximate the benchmark results presented here. We will examine a correction for the LP approximation for diffusive systems with large relative chord lengths and predictions of variance for binary stochastic systems as future research efforts.

Acknowledgements

We would like to thank Brenton Ching for the use of his accelerated transport codes, which were a great contribution in the generation of the benchmark, atomic mix, and Levermore-Pomraning solutions presented. We would also like to thank Richard Sanchez for providing us with an excellent reference [2].

References

1) M.L. Adams, E.W. Larsen, G.C. Pomraning, "Benchmark Results for Particle Transport in a Binary Markov Statistical Medium", *J. Quant. Spectrosc. Radiat. Transfer*, **42**, *4*, 253 (1989).
2) O. Zuchuat, R. Sanchez, I. Zmijarevic, F. Malvagi, "Transport in Renewal Statistical Media: Benchmarking and Comparison with Models", *J. Quant. Spectrosc. Radiat. Transfer*, **51**, *5*, 689 (1994).
3) G.C. Pomraning, *Linear Kinetic Theory and Particle Transport in Stochastic Mixtures*, pp. 85-163, World Scientific Publishing Co., Singapore (1991). A.Z.
4) Akcasu and E.W. Larsen, "A Model of the Scalar Flux Variance for Random Media Transport Problems", *Trans. Am. Soc.*, **89**, 289 (2003).
5) M.L Adams and E.W. Larsen, "Fast Iterative Methods for Discrete-Ordinates Particle Transport Calculations", *Prog. Nucl. Energy*, **40**, 3 (2002).
6) B.S. Ching, and T.S. Palmer, "An Acceleration Scheme for Binary Stochastic Mixture Deterministic Transport in Slab Geometry", *Proceedings of the American Nuclear Society International Meeting on Mathematical Methods for Nuclear Applications*, Salt Lake City, UT (2001).